Detecting Non-Linearity Induced Oscillations via the Dyadic Filter Bank Property of Multivariate Empirical Mode Decomposition

Muhammad Faisal Aftab[a,*], Morten Hovd[a], Selvanathan Sivalingam[b]

[a]*Department of Engineering Cybernetics, NTNU, Trondheim Norway*
[b]*Seimens AS, Trondheim, Norway*

Abstract

Non-linearity induced oscillations in control loops are characterized by the presence of higher order harmonics. In this paper the dyadic filter bank property of the Multivariate Empirical Mode Decomposition (MEMD) is exploited to reveal the harmonic content of the oscillatory signal to indicate the presence of non-linearity. Once the harmonics are identified the extent of non-linearity is evaluated automatically using Degree of non-linearity measure (DNL) introduced in our previous work (Aftab et al., 2016). Although detection of non-linearity via harmonics is an old concept; any automatic method has still not been reported. Moreover, the existing methods suffer from the restrictive assumption of signal stationarity. The proposed method is more robust in identifying the non-linearity induced oscillations and is adaptive and data driven in nature and thus requires no *a priori* assumption about the underlying process dynamics. The proposed method can also differentiate among the different sources of multiple oscillations, for example combinations of nonlinearity and linear sources or two nonlinear sources. Apart from detecting the non-linearities the proposed method can also contribute in locating the source of non-linearity, thereby reducing the maintenance time to a considerable extent. The robustness and effectiveness of the proposed method is established using industrial case studies and results are compared with existing methods based on higher order statistics (Choudhury et al., 2008) and surrogate based methods (Thornhill, 2005).

Keywords: Non-linearity induced oscillations, harmonic content, dyadic

filter bank property, empirical mode decomposition, intra wave frequency modulation

1. Introduction

Oscillations are one of the major causes of degraded control performance in industrial control systems. Product variability, equipment wear, and reduced profitability are the major aftereffects associated with oscillatory control loops. Oscillations can be due to multiple causes like poor controller tuning, disturbances and non-linearities. Non-linearities, ranging from inherent non-linearities in the process itself to ones associated with sensor and actuator faults, are among the major causes of oscillation in industrial control systems. The high complexity and large size of modern industrial processes necessitate the early and correct diagnosis of the oscillation source for timely maintenance and reduced shut down time.

Detection of non-linearity induced oscillations has attracted considerable attention from the research community for more than a decade. Detailed literature reviews can be found in [(Thornhill and Horch, 2007) and (di Capaci and Scali, 2015)], while only a brief overview of some procedures is provided here.

Horch (1999) proposed that an odd correlation between manipulated and process variable indicates the presence of valve non-linearities in non-integrating plants. Other methods based on shape analysis formalisms for detecting valve non-linearities are put forth by Srinivasan et al. (2005), Hägglund (2011) and Yamashita (2005).

Methods pertaining to non-linear time series analysis are also being used by some authors to detect oscillations caused by non-linearities in control loops. One such method, based on higher order statistics (HOS), is put forward by Choudhury et al. (2008). The bi-spectrum of the nonlinearity induced oscillations shows peaks at the corresponding bi-frequencies. Two

*Corresponding author
Email addresses: muhammad.faisal.aftab@itk.ntnu.no (Muhammad Faisal Aftab), morten.hovd@itk.ntnu.no (Morten Hovd)

indices, termed the Non-Gaussianity Index (NGI) and the Non-Linearity Index (NLI), are used to detect the presence of non-linearity. The signal is classified as the output of a linear Gaussian process if NGI $\leq$ 0.0001; whereas NLI$\geq$ 0.01 classifies the signal to be outcome of a non-linear process. Both the NGI and the NLI need to be above their respective thresholds for the signal to be identified as non-linear. In addition, a total non-linearity index (TNLI) is defined to calculate the total non-linearity in the signal. An important limitation for this method is that symmetric waveforms (like square or triangular) exhibiting odd harmonics, cannot be captured [Thornhill (2005) and Zang and Howell (2003)].

Another important method is that of surrogate testing proposed by Thornhill (2005). Surrogates are time series which have exactly the same power spectrum as original time series, but phase is randomized to remove any kind of phase coupling. The algorithm makes use of the fact that the time series from the non-linear source depicts phase coupling and hence is more predictable than its surrogate counterpart. A non-linearity measure called N-measure is defined to accept or reject the null hypothesis that the signal is outcome of a linear Gaussian process. Different parameters like embedding dimensions, the number of nearest neighbors and number of oscillation cycles [1] need to be tuned in order to obtain reliable results.

Non-linearity detection methods based on the Hilbert Huang Transform (HHT) and intra-wave frequency modulation, that are applicable to non-stationary time series, are proposed by Babji et al. (2009) and Aftab et al. (2016). The former gives only the qualitative picture while the latter provides a measure to quantify the severity of non-linearity. The method by Aftab et al. (2016) provides an automatic way to detect non-linearities but it suffers from the inherent mode mixing limitation of Empirical mode decomposition (EMD), the first step in obtaining to the HHT. The mode mixing problem may result in false reporting of the non-linearity in presence of noise and multiple oscillations.

The idea that the oscillations caused by non-linearities contain higher order harmonics is explored by Thornhill et al. (2001). A measure called the

[1] See the original reference for details

distortion factor D is introduced that measures the energy spread among the fundamental frequency and harmonics to detect the extent of non-linearity. This method has certain limitations, the foremost being the manual detection of harmonics and the requirement of stationary data. It is also prone to report inaccurate results in the presence of noise and multiple oscillations due to other causes. This paper is aimed at addressing the limitation of the previous work (Aftab et al., 2016), where the mode mixing problem can result in false detection of non-linearity. In the method proposed here, instead of relying on the intra-wave frequency modulation to classify the time series data, the harmonic content is analyzed using the noise assisted multivariate EMD (MEMD). The presence of harmonics is taken as an indication of non-linearity and then intra-wave frequency modulation is used to measure the extent of non-linearity in the signal.

The advantages offered by the proposed method are threefold. First it removes the mode mixing problem associated with non-linearity detection method given in(Aftab et al., 2016) while retaining the data driven ability of the EMD process. Second, the proposed method is automatic, can sift out the harmonic content adaptively, and can work in the presence of noise and oscillations caused by multiple sources. Third, the extent of non-linearity using intra-wave frequency modulation can help in isolating the source loop of non-linearity.

The paper is organized as follows: Section 2 gives an overview of the EMD, Multivariate EMD and the associated dyadic filter bank property. Section 3 outlines the steps involved in harmonic extraction. The degree of non-linearity and criterion to isolate the non-linearity are discussed in Section 4 and Section 5 respectively. Section 6 gives the detailed algorithm, followed by simulation and industrial case studies in section 7 and 8 respectively, followed by conclusions.

2. Empirical mode Decomposition (EMD) and Variants

2.1. Standard EMD

Standard EMD is also referred to as univariate EMD, as it caters only for one dimensional signals. EMD is a data driven procedure that adaptively

sifts out different components, called Intrinsic Mode Functions (IMFs), from the signal. An IMF is defined as a function that has zero mean and the number of extrema and zero crossings at most differ by one. The method sifts out fast components from the slower ones through an iterative procedure that involves identification of local extrema and fitting an envelope through them using cubic splines. The low frequency components are local means $m(t)$ of the envelope and the local fast component $d(t)$ is then given by [Rilling et al. (2003)]

$$d(t) = x(t) - m(t) \tag{1}$$

The sifting process is repeated until $d(t)$ fulfills the criteria to be an IMF. The IMF is then subtracted from the original signal and the sifting procedure is started again on the residue and continues till no more IMFs are left to be extracted. The signal can then be expressed as the sum of IMFs and residue as

$$x(t) = \sum_{i=1}^{N} c_i(t) + b(t) \tag{2}$$

where $x(t)$ is the input time series, $c_i(t)$ is the i^{th} IMF, $b(t)$ is the residue, and N is the total number of IMFs. The details of the procedure can be found in Huang et al. (1998) and Rilling et al. (2003).

2.2. Multivariate EMD (MEMD)

Given the data driven nature and distinct properties of EMD, efforts were made to extend its applicability to multivariate signals, with the major obstacle to such an extension being the generation of envelope and its mean in the higher dimensions. Rilling et al. (2007) proposed that the envelopes in the 2-dimensional space can be generated by extrema sampling of multiple signal projections in a complex plane. The mean is then calculated by averaging the envelopes from these projections. The projections are calculated using uniformly spaced direction vectors on the unit circle.

Rehman and Mandic (2009) generalized the same concept to n-dimensional signals, the so called Multivariate EMD (MEMD), by generating envelopes in n-dimensional space. The multiple directions are represented by vectors from the center of the unit n-dimensional sphere to the

uniformly distributed points on its surface. The points are generated using uniform sampling by means of Hammersley and Halton sequences.

2.2.1. Hammersley and Halton Sequences

Hammersley and Halton sequences are used to generate low discrepancy sequences for uniform sampling. The kth sample of a one dimensional Halton sequence $\phi_p(k)$ is written as

$$\Phi_p(k) = \frac{a_0}{p} + \frac{a_1}{p^2} + \frac{a_2}{p^3} \dots \frac{a_r}{p^{r+1}} \tag{3}$$

where prime base-p representation of k can be expressed as Wong et al. (1997)

$$k = a_0 + a_1 p + a_2 p^2 \dots a_r p^r \tag{4}$$

where each a_i is an integer in $[0, p-1]$. Starting from $k = 0$ and with $p_1, p_2 \dots p_d$ as d prime numbers, the kth sample of the d-dimensional, Halton sequence then becomes

$$\left(\Phi_{p_1}, \Phi_{p_2}, \dots \Phi_{p_d}\right) \tag{5}$$

A Hammersley sequence can be used when the total number of points (n) are known in advance, thus the kth sample of d-dimensional Hammersley sequence is given by

$$\left(\frac{k}{n}, \Phi_{p_1}, \Phi_{p_2}, \dots \Phi_{p_{d-1}}\right) \quad k = 0, 1 \dots n-1 \tag{6}$$

The Hammersley sequence given by (6) can be used to generate uniform sampling on the unit sphere for envelope generation. The accuracy of the Hammersley sequence may decrease for higher dimensions. This may be improved by using (t, m, s)-nets and (t, s)-sequences (Niederreiter, 1992).

2.3. Envelope and Mean in n-dimensions

The next step is to generate the envelope of all the projection curves, using cubic splines which are in turn averaged to calculate the mean envelope $m(t)$. Fast modes are extracted, in an analogy to the univariate case, by

$d(t) = x(t) - m(t)$ and the procedure is iterated in a similar fashion till there are no more IMFs to extract. The IMFs so generated are also n-dimensional signals, with each dimension corresponding to the corresponding component in the input signal. The detailed algorithm is given in Table 1.

Table 1: Multivariate Empirical Mode Decomposition (MEMD) Algorithm

Algorithm Multivariate EMD

1. Set up K direction vectors ($K = 64$ is used here) u^k with $k = 1 \dots K$ by choosing uniformly spaced points on the n dimensional sphere.
2. Find the projections $p^k(t)$ of the input signal $x(t)$ along the direction vectors u^k for $k = 1 \dots K$.
3. Identify the maxima of projections $p^k(t)$ and corresponding time instants t^k.
4. Generate a multi-variable envelope curve $e^k(t)$ by interpolating $[t^k, x(t^k)]$.
5. The mean of the envelope curve is then given by

$$m(t) = \frac{1}{K} \sum_{k=1}^{K} e^k(t) \tag{7}$$

6. Similar to the univariate EMD, extract local fast mode $d(t)$ from $d(t) = x(t) - m(t)$.
7. Iterate the steps $1 - 5$ on $d(t)$ till it qualifies to be an IMF.
8. Find residue $r(t) = x(t) - d(t)$ and repeat same procedure on the $r(t)$ till all IMFs are extracted.

The uniformly sampled envelope on a three dimensional unit sphere, using the Hammersley points is given in Figure 1.

2.4. Dyadic Filter Bank Property of the MEMD

An important consequence of the MEMD is that it acts like a series of band pass filters in the presence of white noise, analogous to the wavelet

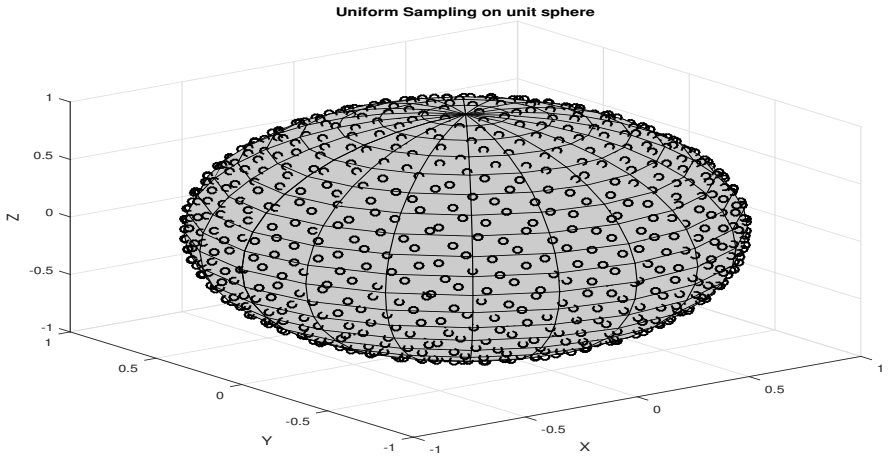

Figure 1: Random sampling with uniform distribution on the unit sphere using the Hammersley sequence

decomposition [Rehman and Mandic (2011)]. This property is referred to as the dyadic filter bank property of MEMD. In order to elaborate this concept an average frequency spectrum of IMFs from 1000 different realizations of three-channel white Gaussian noise is shown in Figure 2. The IMFs can be seen as the output of a series of band pass filters, with the frequency of each band decreasing with the IMF index.

3. Extraction of Harmonics in Univariate Signals

The dyadic filter bank property of MEMD can be enforced on the univariate signals using the so called noise assisted MEMD (NA-MEMD). To achieve this the univariate signal is appended with two or more noise channels to make a multivariate signal which is then processed using the MEMD algorithm. The details of the procedure are discussed next.

3.1. Enforcing the Dyadic Filter Bank Property

The harmonics exhibited by the non-linearity induced oscillations can be extracted by virtue of the dyadic filter bank property of Multivariate EMD. In order to enforce the dyadic filter bank property of MEMD, the

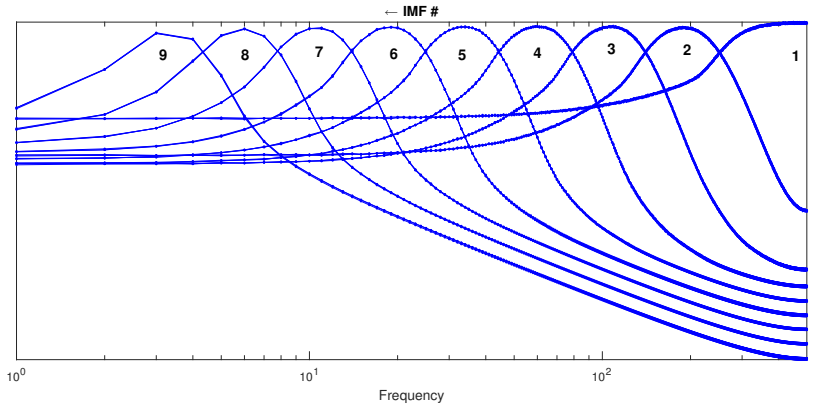

Figure 2: Dyadic Filter Bank property of Multivariate EMD (MEMD),

univariate input signal is appended with two or more noise channels to generate a multivariate signal and thereafter is processed using MEMD algorithm (the detailed steps are described in Table 2) (Rehman et al., 2013). The retained IMFs are univariate (noise channels are discarded) and are aligned according to the filter bank structure. These IMFs are ready to be tested for the presence of harmonics, but first non-significant and noisy IMFs have to be discarded.

3.2. Discarding Spurious and Noisy IMFs

3.2.1. Discarding Pseudo IMFs

The EMD process is prone to produce pseudo IMFs that are poorly correlated with the input signal due to spline fitting issues [Peng et al. (2005), Srinivasan and Rengaswamy (2012) and Aftab et al. (2016)]. The MEMD is also no exception. Therefore in oder to get the significant IMFs, the correlation index of each IMF with original signal is calculated using relation

$$\rho_i = \frac{Cov(c_i, x)}{\sigma_x \sigma_{c_i}}, \quad i = 1, 2, 3 \ldots n \tag{8}$$

where Cov denotes the covariance; σ_x and σ_{c_i} are the standard deviations of the signal and the IMF, respectively, and n is the total number of IMFs.

Table 2: Enforcing dyadic filter bank property

Step 1 Generate two uncorrelated white Gaussian noise sequences with length same as that of the original signal
Step 2 Append the two noise sequences to the original signal to make 3-channel signal, with one channel of original data and two channels of noise
Step 3 Process the signal using Multivariate EMD. The resulting IMFs will have three channels.
Step 4 Retain the IMFs in the channel corresponding to the original signal, and discard the IMF components corresponding to noise channels

The normalized correlation coefficient λ_i is calculated for each IMF

$$\lambda_i = \frac{\rho_i}{max(\rho_i)}, \quad i = 1, 2, 3 \ldots n \tag{9}$$

Only the IMFs with $(\lambda > \eta)$ are retained, where the value of threshold η is discussed in Section 3.4.

3.2.2. Discarding Noisy IMFs

It may happen that, in case of signals with large noise levels, IMFs with large noise content and little information are retained in the previous step. Therefore these noisy IMFs need to be discarded as the objective is to identify the harmonics in the IMFs and these harmonics will have distinct peaks in the frequency spectrum.

To get rid of IMFs consisting mainly of noise, a method based on the sparseness index[Hoyer (2004) and Srinivasan and Rengaswamy (2012)] is used. The frequency spectrum of noise dominated IMFs will be spread across a broad frequency range whereas for oscillatory IMFs it will exhibit distinct peaks. The sparseness index SI of frequency spectrum $X(f)$ of

signal $x(t)$, given by (10) will be almost zero for a noisy signal whereas it will attain a value near one for the oscillatory ones:

$$SI(x) = \frac{\sqrt{N} - \left(\sum_{1=1}^{N} |X_i| / \sqrt{\sum_{1=1}^{N} |X_i|^2} \right)}{\sqrt{N} - 1} \tag{10}$$

Here X is the frequency response and N is total number of frequency channels up to the Nyquist frequency. The IMFs with $SI > S_{Thresh}$, containing distinct peaks, are retained for further analysis. The default value of S_{Thresh} is discussed in Section 3.4.

3.3. Extracting Harmonics

Once the significant and oscillatory IMFs are obtained using the procedure laid down in Section 3.2, the next step is to assess the IMFs for presence of harmonics. The presence of oscillations in retained IMFs and the corresponding time period is determined using the Auto Covariance Function (ACF) method proposed by Thornhill et al. (2003). This is due to the fact that the ACF of an oscillatory signal oscillates with the same frequency with noise confined to zero lag only. The IMFs are converted to the corresponding ACF and zero crossings are evaluated.

If Δt is the time interval between two successive zero crossings, then the average time period $\bar{T}_p$ for n such intervals will be given by [Thornhill et al. (2003) and Srinivasan and Rengaswamy (2012)]

$$\bar{T}_p = \frac{2}{n} \sum_{i=1}^{n} (\Delta t_i) \tag{11}$$

The regularity of the oscillation is determined from the r statistics calculated using the relation

$$r = \frac{1}{3} \frac{\bar{T}_p}{\sigma_{T_p}} \tag{12}$$

where σ_{T_p} is the standard deviation of the the time intervals between zero crossings. The oscillation is detected if $r > 1$ and the mean time period $\bar{T}_p$ is reported.

3.4. Default Parameter Settings

The default settings of different parameters used in this work are outlined in Table 4. The discussion about these default settings, for each parameter, are discussed next.

3.4.1. Number of Zero Crossings

The presence or absence of harmonics is ascertained from the zero crossings of ACF using (11) and (12). Thornhill et al. (2003) recommended to use the first eleven zero crossings for the detection of oscillation. This is so because in the absence of persistent oscillation the auto covariance function decays as a function of lags and may contain spurious zero crossings at large lags. A smaller number of zero crossings tend to make the estimates of $\bar{T}_p$ and σ_p unreliable. Using eleven zero crossings balances these concerns.

3.4.2. Correlation Threshold η

In order to discard the spurious IMFs generated in MEMD process, the normalized correlation coefficient, λ, given in (9), is used. Only the IMFs with $(\lambda > \eta)$ are retained with the threshold η set to 0.25 in this work. This value is chosen such that the IMFs representing significant harmonics can be captured while discarding most pseudo components. The threshold is lower than the value of 0.5 used by Srinivasan and Rengaswamy (2012) because the objective in this work is to capture both the fundamental oscillation as well as the associated harmonics, if they are present.

To elaborate this further consider the example of a square wave with added white noise (shown in the bottom row of Figure 4) which is characterized by the presence of odd harmonics. The average correlation coefficients $\bar{\lambda}$ of extracted IMFs, for 1000 different noise realizations are summarized in Table 3. It is clear that selecting the threshold of 0.25 will enable the proposed method to identify third and fifth harmonics which is sufficient for the purpose of detecting the non-linearity. The chosen threshold is a compromise between the number of higher order harmonics that are discarded and avoiding spurious IMFs that may corrupt the analysis.

Table 3: Correlation coefficient of different IMFs for square wave

IMF	$\bar{\lambda}$	Harmonic
1	0.09	Thirteenth
2	0.14	Eleventh
3	0.16	Ninth
4	0.22	Seventh
5	0.28	Fifth
6	0.33	Third
7	1.00	Fundamental

3.4.3. Sparseness Threshold (S_{Thresh})

In order to extract harmonics, IMFs with sparseness index near to one are retained. In order to get an idea about the value of sparseness index, the spectra of four signals (from industrial data) with different sparseness are shown in Figure 3. The corresponding SI values are given on y-axis. The first row shows the spectrum with harmonic content and has sparseness of 0.67. It can be seen (bottom three spectra) that sparseness index up-to 0.54 may contain spectrum spread across broad frequency range. As we are looking for distinct peaks corresponding to harmonics, the threshold (S_{Thresh}) used in this paper to select the oscillatory IMF can be set as 0.58. The threshold is based on the authors' experience and can be lowered but it will increase the risk of spurious harmonic detection. The effects of changing this threshold on the industrial case study are given in Section 8.

Table 4: Default Parameters Setting

Parameter	Default value
Zero Crossings (n)	11
Correlation Threshold (η)	0.25
Sparseness Threshold (S_{Thresh})	0.58

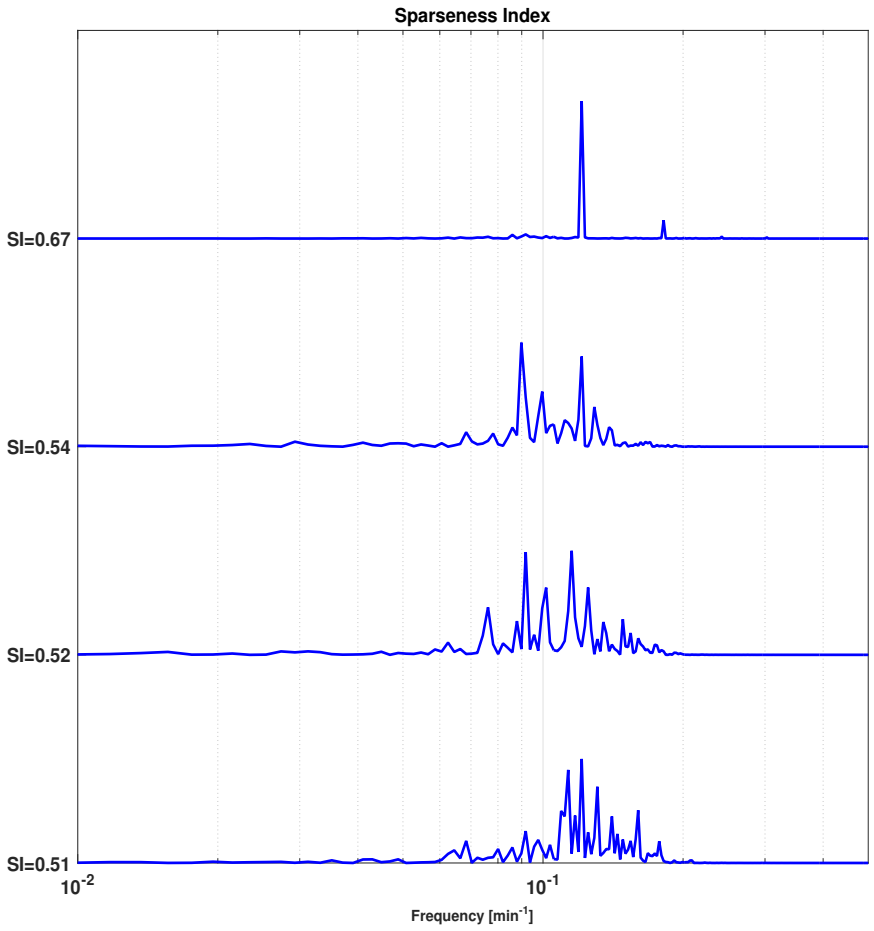

Figure 3: Frequency spectra with sparseness index 0.67(1^{st} row), 0.54 (2^{nd} row), 0.52 (3^{rd} row) and 0.51 (bottom row)

3.5. Automatic Detection of Harmonics

The presence of harmonics is established if there exists mean time periods of IMFs (with $r > 1$) that are integral multiples. The automatic detection of harmonics, the core element of this work, is carried out via following steps

1. Calculate the mean frequency $\bar{\Omega}$ and maximum(minimum) frequency Ω_{max} (Ω_{min}) of oscillation, for each IMF with $r > 1$, using

$$\begin{aligned} \bar{\Omega} &= \frac{1}{\bar{T}_p} \\ \Omega_{max} &= \frac{1}{\bar{T}_p - \sigma_{T_p}} \\ \Omega_{min} &= \frac{1}{\bar{T}_p + \sigma_{T_p}} \end{aligned} \tag{13}$$

2. Identify the most correlated IMF i.e with $\lambda = 1$ and corresponding frequency $\bar{\Omega}_{\lambda_{max}}$.
3. The presence of harmonics is confirmed if oscillations are found at integer multiples of the base frequency; i.e. if for IMF $i, i \in \mathbf{Z}^+$ (different from the fundamental component)

$$\Omega_{max_i} \leq k\bar{\Omega}_{\lambda_{max}} \leq \Omega_{min_i} \quad k > 1 \tag{14}$$

4. In case no harmonics are detected for the most correlated IMF; the steps $2 - 3$ can be repeated for the next most correlated IMF and so on.
5. The condition that the IMF containing the fundamental frequency of oscillation has higher correlation with the actual signal than its harmonics must be fulfilled, to declare two IMFs as a harmonic fundamental pair i.e.

$$\lambda_f > \lambda_{h_i} \quad i \in \mathbf{Z}^+ \tag{15}$$

   where λ_f and λ_{h_i} are the normalized correlation coefficient of fundamental and i^{th}harmonic IMF respectively.
6. Similarly the relation in (15) shall also hold for different harmonics if they arise from the same non-linearity induced oscillation; that is for

k^{th} harmonic.

$$\lambda_{h_k} > \lambda_{h_{k+1}} \quad k \in \mathbf{Z}^+ \tag{16}$$

If two IMFs fulfil (14) ; but not (16), they are considered two different oscillations and not harmonics. This is important to avoid spurious harmonic detection when a signal is affected by multiple sources of oscillation.

The signals whose IMFs exhibit harmonics are then classified as the ones oscillating due to non-linearity. The extent of non-linearity can then be evaluated using the Degree of Non-Linearity (DNL) measure as given in our previous work [Aftab et al. (2016)]. The DNL is based on the concept of intra-wave frequency modulation and instantaneous frequency (IF); a brief overview of these concepts is provided later in section 4.

3.6. Illustrative Example

The rules for harmonic detection outlined in the preceding section can be explained by considering the following illustrative example. Two cases are considered here.

3.6.1. Multiple Oscillations Case

Consider time series data from a closed loop system suffering oscillations due to a combination of a stiction non-linearity and an external sinusoidal disturbance. The fundamental frequency of the stiction nonlinearity is $0.0134 sec^{-1}$ whereas the sinusoidal disturbance has frequency of $0.0067 sec^{-1}$. The simulation model is explained in detail in Section 7 . The oscillatory response of the system is shown in the first row of Figure 4. In total 3 oscillatory modes are identified. The details of these modes are given in Table 5.

It can be seen that first two IMFs form a fundamental harmonic pair with IMF 2 designated as fundamental and IMF 1 as 3^{rd} harmonic according to the rules given in (14-16). It is to be highlighted that the stiction oscillation, in this case, is characterized by the presence of odd harmonics that can not captured by the bi-spectrum (higher order statistics) based method as discussed by Thornhill (2005) and Zang and Howell (2003).

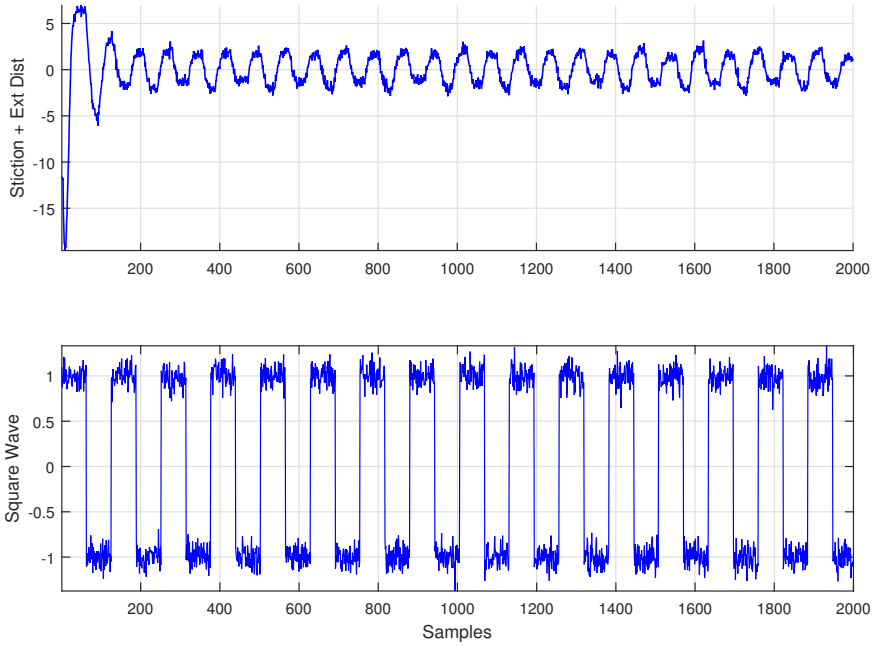

Figure 4: Harmonic detection illustrative example: Stiction plus sinusoidal disturbance (1^{st} row); Square wave (2^{nd} row)

It is to be noted that the 3^{rd} IMF represents the external sinusoidal disturbance, which is regarded as an oscillation separate from the stiction induced oscillation by virtue of the rule given in (16). Thus the proposed algorithm can identify multiple oscillation caused by different sources. Oscillations caused by two different non-linear sources can be detected in a similar fashion.

3.6.2. Symmetric Waves with Odd Harmonics

In order to further establish the fact that the proposed scheme can correctly identify the harmonics in the symmetric waveforms exhibiting odd harmonics the square wave corrupted by white noise of variance 0.1 is considered. The square wave can be seen in the second row of Figure 4. The results summarized in Table 5 show that the proposed method can identify the presence of odd harmonics (3^{rd} and 5^{th}) in the first and second IMFs

with the fundamental frequency residing in the third IMF. The same signal is declared linear by the bi-spectrum based method (NGI=-0.0087).

Table 5: Harmonic detection illustrative example

Dist	IMF	λ	$\bar{\Omega}$	Ω_{min}	Ω_{max}	Harmonics	Type
Ext Dist Plus Stiction	1	0.53	0.0348	0.0278	0.0466	Yes (3^{rd})	Non-Linear
	2	1.0	0.0134	0.0132	0.0137		
	3	0.30	0.0067	0.0062	0.0072	No	Linear
Square Wave	1	0.29	0.0399	0.378	0.0422	Yes (3^{rd}) (5^{th})	Non-Linear
	2	0.32	0.0239	0.0236	0.0243		
	3	1.0	0.0079	0.0079	0.0080		

4. Intra-wave Frequency Modulations and Degree of Non-linearity

4.1. Instantaneous Frequency (IF)

The first step in the computation of the Instantaneous frequency (IF) of the signal is the creation of an analytic signal using the Hilbert transform. The Hilbert transform $Y(t)$ of a signal $X(t)$, also regarded as convolution of $x(t)$ and $1/\pi t$, is given by

$$Y(t) = \frac{1}{\pi} P \int_{-\infty}^{\infty} \frac{X(\tau)}{t-\tau} d\tau = \frac{1}{\pi} P \int_{-\infty}^{\infty} \frac{X(t-\tau)}{\tau} d\tau \tag{17}$$

where P indicates Cauchy's principal value of the integral. The analytic signal $Z(t)$ is then given by

$$\begin{aligned} Z(t) &= X(t) + jY(t) = a(t)e^{j\theta t} \\ a(t) &= \sqrt{X^2(t) + Y^2(t)}, \quad \theta(t) = \arctan \tfrac{Y(t)}{X(t)} \end{aligned} \tag{18}$$

Here the amplitude and phase are functions of time and the instantaneous frequency (IF) is defined as the time derivative of the phase function $\theta(t)$;

given by (Huang et al. (2009))

$$\omega(t) = \frac{d\theta(t)}{dt} = \frac{1}{A^2}[X\dot{Y} - Y\dot{X}] \tag{19}$$

The analytical signal formed in (18) can give the correct IF only if the original signal $X(t)$ fulfills the properties of an IMF. Therefore the IMF generation via EMD is the first step in calculating the IF and this combined procedure of applying EMD and Hilbert transform to arrive at the analytical signal is termed the Hilbert Huang Transform (HHT); further details can be seen in Huang et al. (1998).

4.2. Intra-Wave Frequency Modulation

The non-linearity induced oscillations give rise to intra-wave frequency modulation i.e fluctuation of the IF within one period of oscillation [Huang et al. (1998),Babji et al. (2009),Wang et al. (2012) and Aftab et al. (2016)], and the extent of this modulation can be used to detect and quantify the extent of non-linearity.

A closer look at the filter bank characteristics (Figure 2) reveals an overlapping region among the spectra of adjacent IMFs. This overlapping allows the presence of more than one harmonic within an IMF and hence gives rise to intra-wave frequency modulation.

In order to elaborate this further, consider a signal from industrial data oscillating due to the non-linearity. The power spectrum of the signal is shown in row 1 of Figure 5 with fundamental frequency at $0.06min^{-1}$ and higher harmonics (peaks are shown with red circles). The spectra of extracted IMFs are shown in row 2 of Figure. The fundamental harmonic is shown by the black curve (third IMF). There is some contribution from the second harmonic while there is negligible energy in higher harmonics. The second harmonic (blue curve) primarily rests in the second IMF with some signatures of the fundamental and third harmonics. The third harmonic (red curve) resides in the first IMF, with significant contribution also from the second, fourth and fifth harmonics. Therefore intra wave frequency modulation and hence non-linearity will be highest in the first IMF and lowest in the third IMF. This is quite evident from the IF plots of IMFs

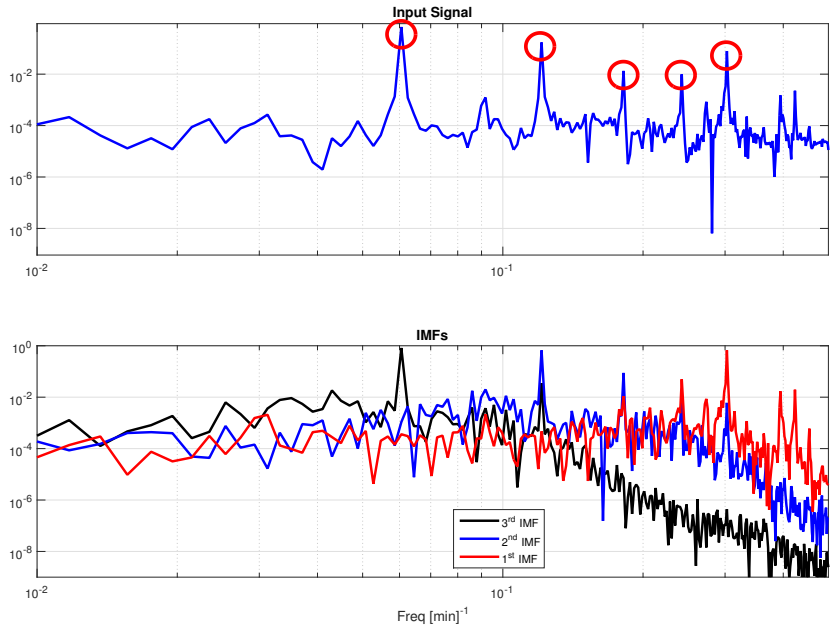

Figure 5: Harmonic content of input signal and corresponding IMFs

in Figure 6. The signal having a higher level of harmonic content will thus have a higher level of non-linearity. The quantification of the extent of non-linearity is given by the degree of non-linearity measure which is explained next.

4.3. Degree of Non-Linearity (DNL) Index

The **Degree of Non-Linearity (DNL)** [Huang et al. (2014) and Aftab et al. (2016)] is the quantification of an extent of non-linearity and is judged by the variation of the IF from its mean value i.e we can write

$$\begin{aligned} DNL &\propto var(IF) \\ DNL &\propto \left\langle \left\{ \frac{IF - IF_z}{IF_z} \right\}^2 \right\rangle^{1/2} \end{aligned} \tag{20}$$

where IF is the instantaneous frequency and IF_z is the full wave zero crossing frequency. The DNL, weighted by the amplitude,for an i^{th} IMF can be

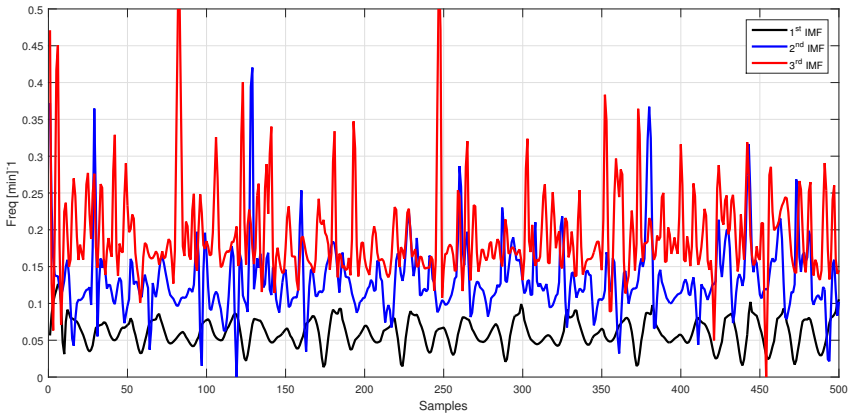

Figure 6: Instantaneous frequency plot for IMFs in Figure 5

defined as [Huang et al. (2014) and Aftab et al. (2016)]

$$DNL_i = std\left\langle \left\{ \frac{IF_i - IF_{z_i}}{IF_{z_i}} \right\} . \frac{a_{z_i}}{\bar{a}_{z_i}} \right\rangle \tag{21}$$

where a_z is the zero crossing amplitude; defined as the absolute value of the extrema between successive zero crossings, $\bar{a}_z$ is the mean of a_z and std is the standard deviation. Equation (21) gives the extent of Non-Linearity in individual IMF; but the **Total Degree of Non-linearity (TDNL)** for the complete signal consisting of N IMFs can be given as sum of individual DNLs weighted by the energy of each IMF. The TDNL is given by [Huang et al. (2014) and Aftab et al. (2016)].

$$TDNL = \sum_{j=1}^{N} \left\langle DNL_j \frac{|c_j|^2}{\sum_{k=1}^{N} |c_k|^2} \right\rangle \tag{22}$$

Here $|c_j|^2$ is the 2-norm of the j^{th} IMF.

5. Isolating the Source of Non-Linearity

Once the control loops suffering from the non-linearity induced oscillations are identified, the next step is to isolate the source for targeted main-

tenance and remedial actions. In a multi loop environment non-linearity induced oscillations at one point may propagate to other variables so the correct diagnosis will reduce the shut down time and cost of repair. Thornhill (2005) pointed out that the different parts of a plant tends to behave as low pass mechanical filters and thus filter out the higher harmonics as we move away from the source of non-linearity.

The TDNL measure discussed in section 4.3 can be used to compare the extent of non-linearity in different variables. The loop with maximum TDNL value is taken to be the source of non-linearity. In section 8, the proposed method is illustrated using the industrial data and results are compared with the existing methods.

6. Proposed Method

The detailed steps for the proposed method for the identification and isolation of the non-linearity induced oscillations are listed below.

1. Follow steps 1-4 (Table 2) to enforce the dyadic filter bank property.
2. Retain the IMFs that are correlated to the original signal and are sparse as per the criterion in Section 3.2.
3. Calculate the ACF of the retained IMFs
4. Identify the zero crossings of individual ACFs and calculate the mean time period $\bar{T}_p$ and regularity statistics r
5. Report the $\bar{T}_p$ of all the IMFs with $r > 1$.
6. Check for the presence of harmonics using the steps described in Section 3.5
7. Report non-linearity if harmonics are present.
8. Compute the DNL and TDNL measures of the IMFs representing fundamental and harmonics
9. The loop with maximum TDNL value is taken as the source of non-linearity induced oscillation.
10. In case of multiple sources of non-linearity induced oscillations, steps 7 to 9 are repeated for each fundamental/ harmonics pair.

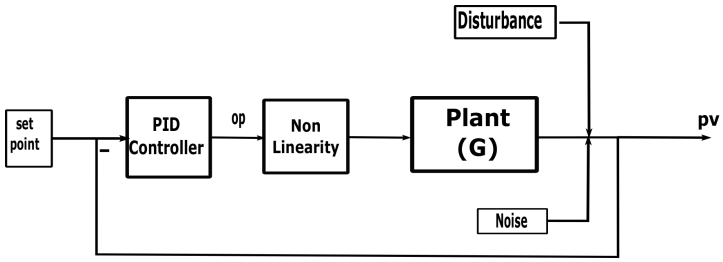

Figure 7: Closed loop system (simulation example)

7. Simulation Example

The simulation example is taken form our recent work Aftab et al. (2016); where oscillations from different sources in a SISO feedback system are analyzed using the proposed method to look for signatures of harmonics or non-linearities. The feedback system is shown in Figure 7. The non-linearity is modeled by stiction using the two parameter model by Choudhury et al. (2008) with $S = 7$ and $J = 5$. The plant dynamics are given by

$$G(s) = \frac{2.25}{4.54s + 1} e^{-3s} \tag{23}$$

Nominal PI controller gains are $K_c = 0.1$ and $K_i = 0.05$. Noise with variance 0.1 is added to test the robustness of the proposed scheme.

In total five test cases, using plant output or process variable (pv) data, are considered for analysis and the results are explained next. It is to be highlighted that the transient effects are included in the analysis that induces non-stationarity. Moreover, a special test case with time varying drift is also introduced to test the robustness of the proposed scheme against stronger non-stationarity. The results for all test case are summarized in Table 6. The DNL and $TDNL$ measures for the simulation example are given in Table 7.

7.1. External Disturbance

In this case the feedback system is subjected to an external sinusoidal disturbance. The system response is shown in the first row of Figure 8.

The results show absence of harmonics thereby attributing the oscillations to a linear cause.

7.2. External Disturbance and Poor Tuning

In this scenario the oscillations resulting from the combination of poor controller tuning and external sinusoidal disturbance are analyzed. The time trend for this case is shown in the second row of Figure 8. The results show absence of any harmonics thus concluding that oscillation are caused by linear source.

7.3. Non-linearity/Stiction

In this case oscillations induced due to non-linearity effects, modeled by stiction in the control valve, are analyzed. The time trend for this scenario is shown in the third row of Figure 8. The results clearly indicate presence of harmonics in the oscillatory signal. It is to be noted that the oscillations are characterized by odd harmonics as third (3^{rd}) harmonic is identified along with the fundamental. This case of stiction induced oscillation cannot be captured by the HOS based non-linearity detection method. The value of Non Gaussianity Index $NGI = -0.01$ confirms this fact.

7.4. Stiction and External Sinusoidal Disturbance

In this case an external sinusoidal disturbance is added to the system with stiction non-linearity. The same case is reported in the illustrative example of Section 3.5. The results clearly show that the proposed method has been able to separate the external sinusoidal disturbance from the stiction induced oscillation. Moreover the proposed rules make it possible to treat the sinusoidal disturbance as separate oscillation from the stiction.

7.5. Sinusoidal Disturbance with Time Varying Set Point

In order to test the robustness of the proposed scheme against non stationary effects, the system is subjected to a time varying set point in the form of ramp signal and an external sinusoidal disturbance. The system response, given in the last row of Figure 8, clearly shows the non-stationary effects. The proposed scheme separates out the sinusoidal disturbance from

the time varying component, with the latter extracted in the residue $b(t)$ (2). The results for this case show the presence of only one oscillatory component void of any harmonics.

Table 6: Nonlinearity detection simulation example

Case	IMF	λ	$\bar{\Omega}$	Ω_{min}	Ω_{max}	Harmonics	Type
Ext Dist	1	1.0	0.0159	0.0156	0.0163	No	Linear
	2	0.35	0.010	0.0085	0.013		
Ext Dist + Poor Tuning	1	1.0	0.083	0.083	0.083	No	Linear
	2	0.5	0.0159	0.0157	0.0162		
Stiction	1	0.54	0.0353	0.027	0.0506	Yes (3^{rd})	Non-Linear
	2	1.0	0.0135	0.0134	0.0137		
Ext Dist Plus Stiction	1	0.53	0.0348	0.0278	0.0466	Yes (3^{rd})	Non-Linear
	2	1.0	0.0134	0.0132	0.0137		
	3	0.30	0.0067	0.0062	0.0072	No	Linear
Ext Dist + Time Varying Set Point	1	1.0	0.0159	0.0156	0.0161	No	Linear

Table 7: DNL and TDNL for simulation example

Case	Type	IMF	DNL	$TDNL$
Ext Dist	Linear(no harmonics)	–	–	–
Ext Dist Poor Tuning	Linear (no harmonics)	–	–	–
Stiction	Non-Linear	1	0.29	0.11
		2	0.1	
Stiction + Ext Dist	Non-Linear	1	0.33	0.11
		2	0.1	
Ext Dist + Time Varying Set Point	Linear(no harmonics)	–	–	–

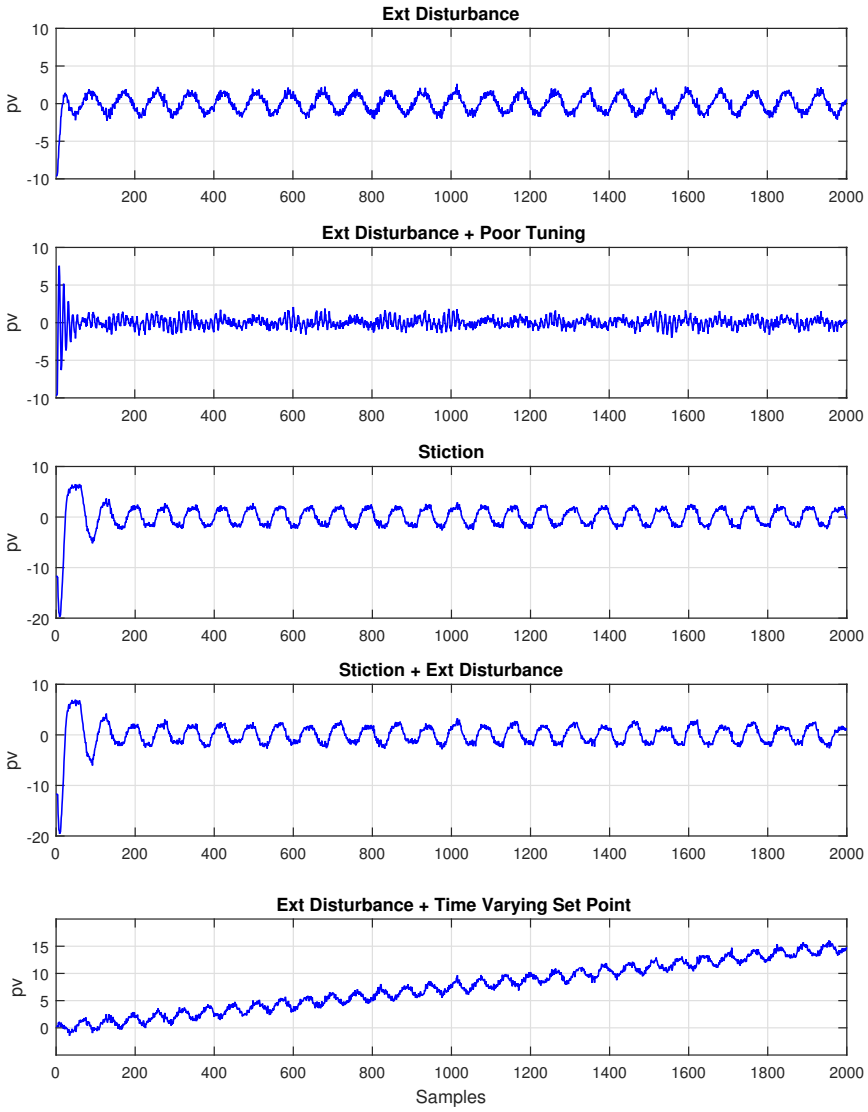

Figure 8: Time trends for simulation example

7.6. Robustness with Increasing Noise Variance

The robustness of the proposed method against noise levels is studied by varying the noise variance for the five simulation test cases. The noise variance σ_v^2 is varied from $\sigma_v^2 = 0.2$ to $\sigma_v^2 = 1.0$ in steps of 0.2. A graphical representation of the results are provided in Figure 9. It can be seen that proposed method is quite robust and can work well even with increased noise variance. In only two cases the reported results are erroneous, both occurring at a large noise variance of $\sigma_v^2 = 1.0$ with SNR of around 2dB.

8. Industrial Case Study

The case study is taken from Thornhill (2005) and Zang and Howell (2005), where a group of variables from a South East Asian refinery are found to be oscillating with the same fundamental frequency of $0.06 min^{-1}$. It has been reported that the plant-wide oscillation stems from the the sticking valve in one of the control loops. Thus the aim is to find the variables that exhibit non-linearity induced oscillations and hence can be regarded as the source of oscillations. The results of the proposed method are compared with those obtained by the HOS based method and surrogate based methods for the same case study. The time trends (plotted in Figure 10) of the process variables (pv), recorded at 1 minute sample rate, are used for the analysis.

8.1. Non-linearity Detection in Individual Loops

The group consisting of 12 variables (shown in first column of Table 8 is analyzed using the proposed method and the results are summarized in Table 8 ; whereas comparison with HOS based method ((Choudhury et al., 2008),(Choudhury, 2006)) and surrogate based method (Thornhill, 2005) are given in Table 9.

The proposed method has identified four loops containing the signatures of non-linearity, namely Tags 11, 24, 33 and 34. In addition to the identification of harmonics the proposed method has been able to identify the presence of multiple oscillations in different tags. For instance low frequency oscillations, other than plant wide oscillation, in Tags 11, 19 and 25 are also detected.

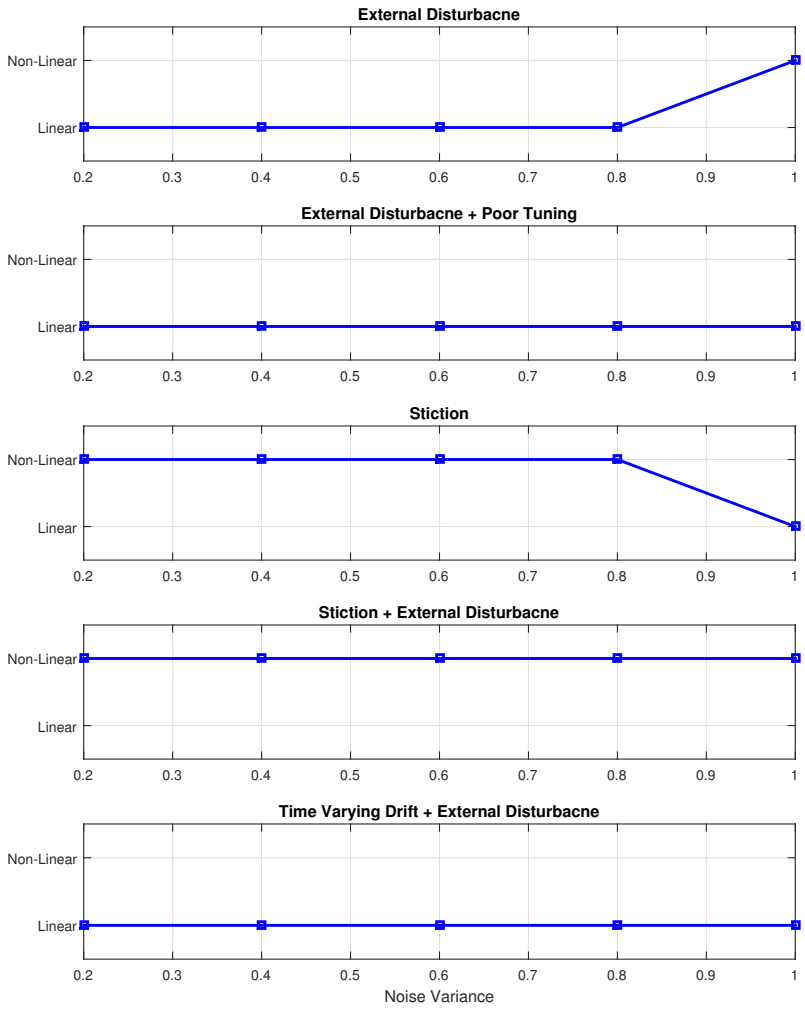

Figure 9: Performance of proposed method for increasing noise levels

Table 8: Non-Linearity detection industrial case study

Tag	IMF	λ	$\bar{\Omega}$	Ω_{min}	Ω_{max}	Harmonics	Type
2	1	1.0	0.0604	0.0572	0.0641	No	Linear
3	1	1.0	0.0604	0.0572	0.0641	No	Linear
4	1	0.49	0.0696	0.0548	0.0954	no	Linear
	2	1.0	0.0604	0.0572	0.0641		
	3	0.32	0.0201	0.0181	0.0226		
10	1	1.0	0.0604	0.0572	0.0641	no	Linear
11	1	0.30	0.1833	0.1565	0.2212	Yes	Non-Linear
	2	0.47	0.1222	0.0993	0.1589		
	3	1.0	0.0604	0.0572	0.0641		
	4	0.59	0.0120	0.0104	0.0142		
13	1	0.66	0.2750	0.2250	0.3537	No	Linear
	2	1.0	0.0604	0.0572	0.0641		
19	1	1.0	0.0604	0.0572	0.0641	No	Linear
	2	0.49	0.0163	0.0129	0.0219		
	3	0.41	0.0121	0.0111	0.0132		
20	1	1.0	0.0604	0.0572	0.0641	No	Linear
24	1	0.80	0.1122	0.1005	0.1272	Yes	Non-Linear
	2	1.0	0.0604	0.0572	0.0641		
25	1	1.0	0.0604	0.0572	0.0641	No	Linear
	2	0.32	0.0275	0.0264	0.0287		
	3	0.29	0.0168	0.0139	0.0212		
33	1	0.75	0.122	0.1138	0.1319	Yes	Non-Linear
	2	1.0	0.0604	0.0572	0.0641		
34	1	0.42	0.2895	0.2279	0.3968	Yes	Non-Linear
	2	0.52	0.1222	0.1080	0.1408		
	3	1.0	0.0604	0.0572	0.0641		

Table 9: Comparison of proposed and existing non-linearity measures

Tag	Proposed Method			HOS			N
	IMF	DNL	TDNL	NGI	NLI	TNLI	(surrogate)
Tag 2	–	–	–	0.15	0.99	2.71	–
Tag 3	–	–	–	0.14	0.94	2.65	–
Tag 4	–	–	–	0.06	0.81	0.81	–
Tag 10	–	–	–	0.04	0.79	0.79	–
Tag 11	1	0.32	0.09	0.20	0.96	2.84	2.74
	2	0.22					
	3	0.06					
Tag 13	–	–	–	0.15	0.96	1.80	2.64
Tag 19	–	–	–	0.13	0.88	0.88	–
Tag 20	–	–	–	0.13	0.94	1.76	–
Tag 24	1	0.197	0.12	0.01	0.76	0.76	–
	2	0.099					
Tag 25	–	–	–	0.0	0.0	0.0	–
Tag 33	1	0.23	0.13	0.080	0.87	3.32	2.57
	2	0.09					
Tag 34	1	0.53		0.20	0.99	7.63	4.91
	2	0.27	0.31				
	3	0.27					

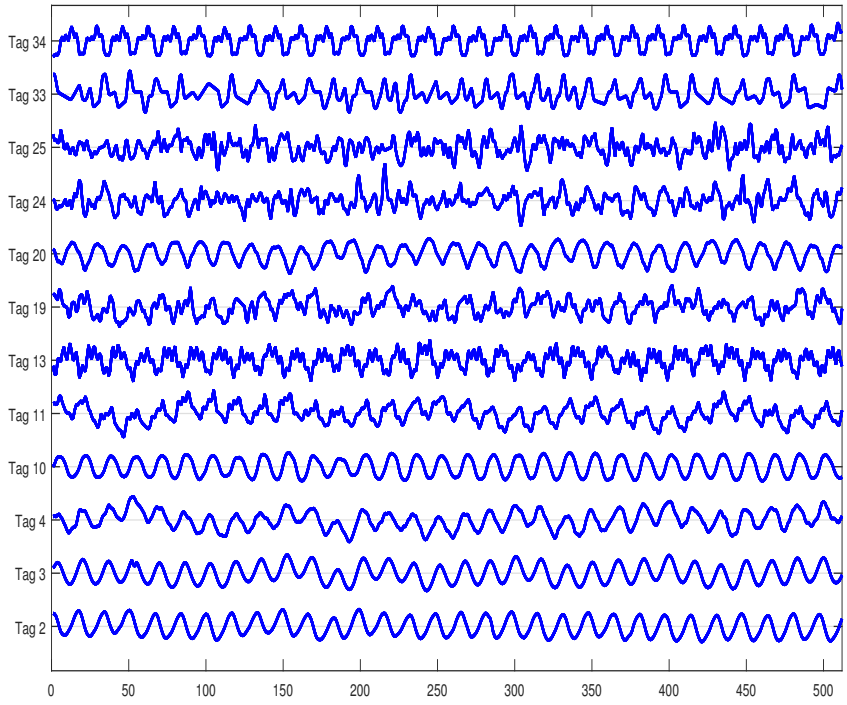

Figure 10: Time trends for the group of variables oscillating with frequency $0.06min^{-1}$ for SEA refinery

8.2. Isolating the Source of Non-Linearity

Once the variables oscillating due to a non-linear cause are identified the next logical step is to isolate the non-linearity to reduce the critical maintenance and shut down time. As discussed in section 5 the non-linearity signature diminishes as we move away from the source of the non-linearity due to mechanical filtering of the higher order harmonics. Therefore the loop with the highest value of the non-linearity measure is candidate for the source of non-linearity.

The TDNL measure given in Table 9 shows that Tag 34 exhibits greatest non-linearity and hence is the most probable candidate for the root cause. Similar results are reported by both HOS based method Choudhury (2006) and surrogate method Thornhill (2005). The proposed method places Tag 33 as the second most non-linear one due to greater energy of higher order harmonics (same as in HOS based method); whereas the surrogate analysis ranks it lower than Tag 11 and Tag 13.

The provision of flow diagrams and P&IDs can make the analysis more accurate by taking considerations based on the physical structure of the plant into account. However, some companies may be reluctant to make such documentation available to external consultants, and the aim of this work has been to develop an analysis technique based on the on-line measurements alone.

8.3. Effect of Changing Correlation and Sparseness Thresholds

The effect of changing the thresholds both for normalized correlation coefficient η and sparseness index S_{Thresh} are analyzed and the results for both cases are given in Figures 11 and 12 respectively. The correlation threshold is varied from 0.15-0.35 whereas the sparseness threshold is varied from 0.55-0.62. It can be seen that the results are mostly stable with respect to these variations. The only exception are Tags 11 and 24 whose harmonic content is lost if the sparseness threshold increases beyond 0.60.

8.4. Comparison with other Methods

The results are quite comparable with the surrogate based non-linearity detection method with the exception of only Tags 13 and 24. Tag 13 comes

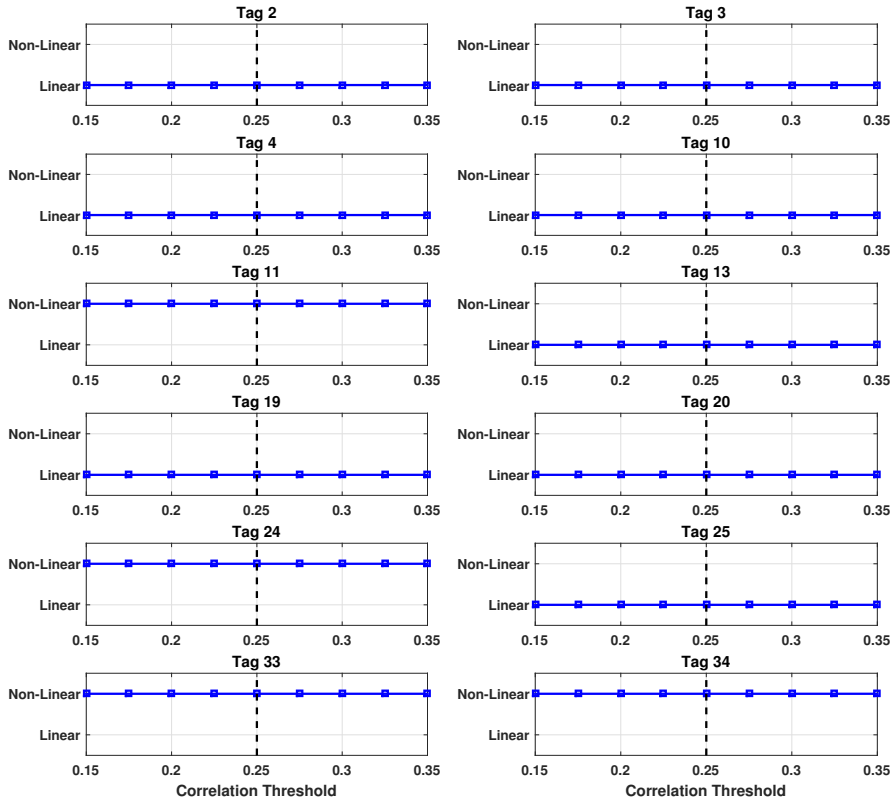

Figure 11: Effect of changing correlation threshold (η) for industrial case study ; vertical dashed line shows default value

out to be linear in the proposed method because the oscillations in the IMF representing the second harmonic were not regular; giving the regularity index $r = 0.7$. The reason is the presence of some other oscillations with the second harmonic in that frequency range. Tag 24, because of presence of harmonics, is declared non-linear, similar to the results of the HOS method which reports it to have quite significant non-linearity with NLI= 0.76. The amplitude of Tag 24 is very small and both Tag 13 and Tag 24 are considered ambiguous in the analysis by Zang and Howell (2005) as well.

The HOS based method declares all the loops with the exception of Tag 25 as non-linear. This finding is substantiated by neither the method proposed

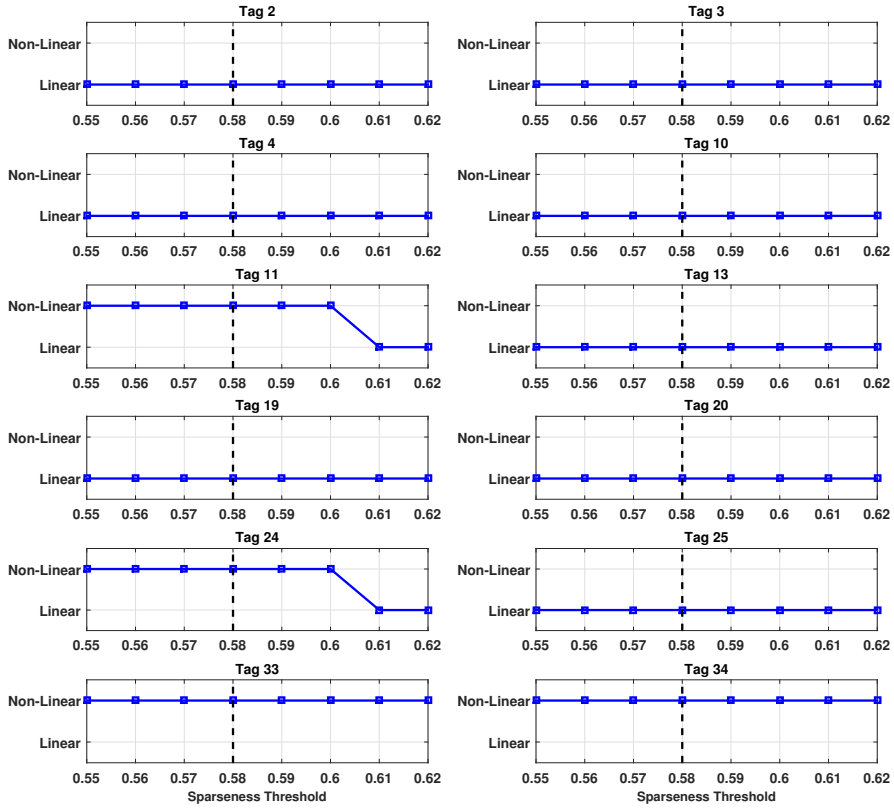

Figure 12: Effect of changing sparseness index threshold (S_{Thresh}) for industrial case study ; vertical dashed line shows default value.

in this paper nor the surrogate analysis. Thus apart from not being able to capture the nonlinearities characterized by odd harmonics, the HOS based method appears to classify too many signals as non-linear.

As far as the comparison with harmonic distortion factor by Thornhill et al. (2001) is concerned, it was pointed out by the authors themselves that the method is based on manual detection of harmonics and can be misleading in presence of noise and multiple oscillations. Tag 25 is shown to have high distortion factor owing to the presence of noise. This shortcoming is totally removed in the proposed method where automatic harmonic

detection is performed and Tag 25 is correctly diagnosed as not containing any nonlinearity signatures.

9. Conclusions

This paper presents a method, based on noise assisted MEMD, to identify the harmonics and hence non-linearity in control loops. The method is adaptive in nature with no *a priori* assumptions about the underlying signal or the process itself. The method can extract harmonics in the presence of noise and multiple oscillations and hence identify the presence of non-linearity. The extent of non-linearity is then calculated via intra-wave frequency modulation and quantified using the total degree of non-linearity measure (TDNL). Results of the proposed method are compared with the HOS and surrogate based methods and are comparable with the surrogate analysis method both in terms of detection and isolation of non-linearity.

10. Acknowledgments

This work is being funded by Siemens AS, Norway. The fruitful discussions with Prof Nina F. Thornhill (Imperial College London) regarding the calculation of $N-$ measure are gratefully acknowledged. Moreover, the authors would like to thank Prof A.K. Tangirala (IIT Madras) for the provision of industrial data.

11. References

Aftab, M. F., Hovd, M., Huang, N. E., Sivalingam, S., 2016. An adaptive non-linearity detection algorithm for process control loops. IFAC-PapersOnLine 49 (7), 1020 – 1025.

Babji, S., Gorai, P., Tangirala, A. K., 2009. Detection and quantification of control valve nonlinearities using hilbert–huang transform. Advances in Adaptive Data Analysis 1 (03), 425–446.

Choudhury, A. A. S., Shah, S. L., Thornhill, N. F., 2008. Diagnosis of process nonlinearities and valve stiction: data driven approaches. Springer Science & Business Media.

Choudhury, M. S., 2006. Troubleshooting plantwide oscillations using nonlinearity information. Journal of Chemical Engineering, 50.

di Capaci, R. B., Scali, C., 2015. Review on valve stiction. part i: From modeling to smart diagnosis. Processes 3 (2), 422.
URL http://www.mdpi.com/2227-9717/3/2/422

Hägglund, T., 2011. A shape analysis approach for diagnosis of stiction in control valves. Control Engineering Practice 40, 782–789.

Horch, A., Oct. 1999. A simple method for detection of stiction in control valves. Control Engineering Practice 7(10), 6708–6718.

Hoyer, P. O., 2004. Non-negative matrix factorization with sparseness constraints. The Journal of Machine Learning Research 5, 1457–1469.

Huang, N. E., Lo, M.-T., Zhao-Hua, W., Xian-Yao, C., May 20 2014. Method for quantifying and modeling degree of nonlinearity, combined nonlinearity, and nonstationarity. US Patent 8,732,113.

Huang, N. E., Shen, Z., Long, S. R., Wu, M. C., Shih, H. H., Zheng, Q., Yen, N.-C., Tung, C. C., Liu, H. H., 1998. The empirical mode decomposition and the hilbert spectrum for nonlinear and non-stationary time series analysis. R. Soc. Lond. A 454, 903–995.

Huang, N. E., Wu, Z., Long, S. R., Arnold, K. C., Chen, X., Blank, K., 2009. On instantaneous frequency. Advances in adaptive data analysis 1 (02), 177–229.

Niederreiter, H., 1992. Random number generation and quasi-Monte Carlo methods. SIAM.

Peng, Z., Peter, W. T., Chu, F., 2005. A comparison study of improved Hilbert Huang transform and wavelet transform: application to fault diagnosis for rolling bearing. Mechanical systems and signal processing 19 (5), 974–988.

Rehman, N., Mandic, D. P., 2009. Multivariate empirical mode decomposition. In: Proceedings of The Royal Society of London A: Mathematical, Physical and Engineering Sciences. The Royal Society, p. rspa20090502.

Rehman, N. U., Mandic, D. P., 2011. Filter bank property of multivariate empirical mode decomposition. Signal Processing, IEEE Transactions on 59 (5), 2421–2426.

Rehman, N. U., Park, C., Huang, N. E., Mandic, D. P., 2013. EMD via MEMD: Multivariate noise-aided computation of standard emd. Advances in Adaptive Data Analysis 5 (02), 1350007.

Rilling, G., Flandrin, P., Gonçalves, P., Lilly, J. M., 2007. Bivariate empirical mode decomposition. Signal Processing Letters, IEEE 14 (12), 936–939.

Rilling, G., Patrick, F., Paulo, G., 2003. On empirical mode decomposition and its algorithms. IEEE-EURASIP workshop on nonlinear signal and image processing 3, 8–11.

Srinivasan, B., Rengaswamy, R., 2012. Automatic oscillation detection and characterization in closed-loop systems. Control Engineering Practice 20 (8), 733–746.

Srinivasan, R., Rangaswamy, R., Miller, R., 2005. Control loop performance assessment. 1. a qualitative approach for stiction diagnosis. Industrial Engineering Chemistry Re-

search 44, 6708–6718.

Thornhill, N., Shah, S., Huang, B., 2001. Detection of distributed oscillations and root-cause diagnosis. In: Proceedings of CHEMFAS 4, june 7-8, Jejudo (Chejudo) Island, Korea. pp. 167–172.

Thornhill, N. F., 2005. Finding the source of nonlinearity in a process with plant-wide oscillation. Control Systems Technology, IEEE Transactions on 13 (3), 434–443.

Thornhill, N. F., Horch, A., 2007. Advances and new directions in plant-wide disturbance detection and diagnosis. Control Engineering Practice 15 (10), 1196–1206.

Thornhill, N. F., Huang, B., Zhang, H., 2003. Detection of multiple oscillations in control loops. Journal of Process Control 13 (1), 91–100.

Wang, Y., Wang, H., Zhang, Q., Aug. 2012. Non-linear distortion identification based on intra-wave frequency modulation. An International Journal of Applied Mathematics and Information Sciences 15(5), 505–514.

Wong, T.-T., Luk, W.-S., Heng, P.-A., 1997. Sampling with hammersley and halton points. Journal of graphics tools 2 (2), 9–24.

Yamashita, Y., 2005. An automatic method for detection of valve stiction in process control loops. Control Engineering Practice 14, 503–510.

Zang, X., Howell, J., 2003. Discrimination between bad tuning and non-linearity induced oscillations through bispectral analysis. In: SICE 2003 Annual Conference. Vol. 1. IEEE, pp. 896–900.

Zang, X., Howell, J., 2005. Isolating the root cause of propagated oscillations in process plants. International Journal of Adaptive Control and Signal Processing 19 (4), 247–265.